A Novel Predictive Model Associated With Osteosarcoma Metastasis

Han Zhang
Shandong Province
Guanhong Chen
Shandong Province
Xiajie Lyu
Weifang Medical University
Tao Li
Qingdao University
Rong Chun
Qingdao University
Yingzhen Wang
Qingdao University
Ying Xu
Shandong Province
Chengyu Lyu (✉ 18266390138@163.com)
Qingdao University

Research

Keywords: lncRNAs, osteosarcoma, tumor metastasis, prognosis

Posted Date: June 15th, 2021

DOI: https://doi.org/10.21203/rs.3.rs-597836/v1

Abstract

Background: Long non-coding RNAs (lncRNAs) have diverse roles in modulating gene expression on both transcriptional and translational aspects, whereas its role in the metastasis of osteosarcoma (OS) is unclear.

Method: Expression and clinical data were downloaded from TARGET datasets. The OS metastasis model was established by seven lncRNAs screened by univariate cox regression, lasso regression and multivariate cox regression analysis. The area under receiver operating characteristic curve (AUC) values were used to evaluate the models.

Results: The predictive ability of this model is extraordinary (1 year: AUC = 0.92, 95% CI = 0.83–1.01; 3 years: AUC = 0.87, 95% CI = 0.79–0.96; 5 years: AUC = 0.86, 95% CI = 0.76–0.96). Patients in high group had poor survival compared to low group ($p < 0.0001$). “NOTCH_SIGNALING”, and “WNT_BETA_CATENIN_SIGNALING” were enriched via the GSEA analysis and dendritic cells resting were associated with the AL512422.1, AL357507.1 and AC006033.2 ($p < 0.05$).

Conclusion: We constructed a novel model with high reliability and accuracy to predict the metastasis of OS patients based on seven prognosis-related lncRNAs.

Introduction

OS is the most common primary malignant bone tumor [1]with a bimodal age distribution. The first peak is during adolescence and the second peak is in older adulthood. [2–6]. With the development of treatments, surgery and multiagent intensive chemotherapy were the mainstream strategies [7–9]. The high rate of metastasis in OS, especially lung metastasis, leads to a poor prognosis [10–12]. The 5-year overall survival rate is about 75% for nonmetastatic OS; however, it is only 20% for metastatic cases [13,14]. Thus, it is necessary to develop biomarkers for early detection and treatment.

LncRNA is a non-coding RNA that ranges from nearly 200 nucleotides (nt) to over 100 kilobases (kb) in length [15]. LncRNA modulates gene expression on both transcriptional and translational aspects, including chromosome rearrangement, histone modification, alternative splicing formation and RNA stabiliziation[16]. LncRNA has been elucidated to play a role in tumor differentiation, invasion, and metastasis [17–21]. LncRNA is involved in the initiation and progression of metastasis of cancer. For example, MALAT1 regulated the metastasis of lung cancer mainly through epithelial-mesenchymal transition (EMT) [22,23]. It was also reported as a metastasis promoter in bladder cancer by activating Wnt signaling [24,25]. HOTAIR promoted pancreatic cancer metastasis via suppressing interferon-related genes [26]. MEG3 has a decisive role in meningioma and gastric cancer through adjusting the autophagy and DNA repair [27,28]. However, the role of lncRNA in OS remains unclear, and a lncRNA-based prediction model is still unavailable yet.

Advances in high-throughput technologies enable researchers to identify the biomarkers and construct the predictive model for customized cancer treatments. In this study, we want to put forward a new risk-score model to predict the metastasis of OS patients using lncRNAs. Furthermore, we would detect the critical biological process, immune-related cells and immune checkpoint.

Method

Target Data and Processing

The clinical information and expression profiles, including mRNA and lncRNA expression profiles, were downloaded from the TARGET datasets (https://ocg.cancer.gov/programs/target). All datasets were subjected to standardized data preprocessing. A total of 22 metastasis and 66 primary OS tissue-related information was analyzed in this study. Pre-processing of the data was performed via RStudio, including background correction, normalization and batch effect adjustment.

Feature Selection and Construction of Prognostic Model

Firstly, differential gene expression of 22 metastasis and 66 primary OS patients containing lncRNA and mRNA was obtained and compared using the Limma R package. P-value 0.05 and |log 2 (fold change [FC])| >1 were set as the threshold criteria. Univariate cox regression, the least absolute shrinkage and selection operator (LASSO) regression and multivariate cox regression analysis were further used to screen the differentially expressed lncRNA in the present study by survival and glmnet R packages. The lncRNA-based prognosis risk score was established based on a linear formula with the expression level multiplied regression model (β). The median risk score was utilized to divide patients into the high-risk group and the low-risk group. Kaplan–Meier (KM) survival and receiver operating characteristic (ROC) curves were plotted by survival and survival ROC R packages.

Scale-Free Co-Expression Network and enrichment analysis

To reconstruct the scale-free co-expression network, prognosis-related lncRNAs and metastasis-related mRNA were utilized. 24 metastasis-related mRNA related to 7 metastasis-related lncRNAs (correlation coefficient $R>0.3$, $p<0.001$) were chosen. The software Cytoscape was used for network visualization. We also analysis the interactions between 24 metastasis-related mRNA and transcription factor (TF) using the DAVID. GO pathway enrichment analyses were performed using the R package clusterProfiler. $P<0.05$ served as a cut-off of statistical significance.

Gene Set Enrichment Analysis and Gene Set Variation Analysis

Gene set enrichment analysis (GSEA) was conducted using GSEA2.2.4 software to generate an enrichment score. The gene sets used for the enrichment analysis were downloaded from the Molecular Signatures Database (MsigDB). Gene sets with a false discovery rate (FDR) value less than 0.05 after performing 1000 permutations were significantly enriched.

Gene Set Variation Analysis (GSVA) is a method to estimate the variation of gene set enrichment through the samples of expression data set. GSVA was performed with the GSVA package (from R Project 3.5.1) of R software with default parameters using the Hallmark gene set.

Infiltrating Immune Cells

The CIBERSORT algorithm was utilized to assess the 22 kinds of immune cell types in metastasis and primary OS group. Next, we analyze the association between 7 prognosis-related lncRNAs and immune cells.

Cell lines and qPCR

Highly metastasis human OS cell lines (MNNG) and weakly metastasis human OS cell lines (U2S2, SAOS-2, SJSA-1 and HOS) were purchased from iCell (Shanghai, China). Total RNA was isolated using Trizol (Invitrogen Life Technologies). cDNA was amplified via PrimeScript RT Master Mix (Takara). The primers used were shown in TableS1.

Result

Differential Gene and lncRNA Screening

22 metastasis and 66 primary OS samples were utilized in this study. To select differential genes and lncRNA, the Limma R package was adopted. As a result, 135 differential lncRNAs were identified, including 79 upregulated and 56 downregulated ***(Figure 1A)***. In addition, there were 171 differential genes ***(Figure 1B)***.

Construction of Prognosis Assessment Model

The results of the univariate cox regression analysis of 135 lncRNAs were used in the LASSO regression to identify robust markers. After the multivariate cox analysis, we identified seven prognosis-related lncRNAs ***(Figure 2A-C)***, which consisted of AL512422.1, AL008718.3, C5orf66-AS1, AL360182.2, CEBPA-DT, AC006033.2 and AL357507.1. All of these lncRNAs were taken part in prognosis model establishing, namely, y= 2.603*AL512422.1+3.735*AL008718.3+18.047* C5orf66-AS1+1.292*AL360182.2+0.475*CEBPA-DT+0.038* AC006033.2 +1.812*AL357507.1. The patients were divided into a high-risk and low-risk group based on the median risk score calculated by the above formula. The expression of seven prognosis-related lncRNAs in high and low-risk groups was depicted in Figure 2D. Moreover, the model performed stronger prediction power and all area under the curve (AUC) values were all >0.8 1 year: AUC = 0.92, 95% CI = 0.83–1.01; 3 years: AUC = 0.87, 95% CI = 0.79–0.96; 5 years: AUC = 0.86, 95% CI = 0.76–0.96) (***Figure 2D***). According to KM survival curves ***(Figure 2D)***, the high-risk group had significantly poor overall survival time compared with the low-risk group (p<0.0001, HR=1.09, 95% CI = 1.06-1.13). In addition, the KM survival curves suggested that five lncRNAs, including AL512422.1, AL008718.3, C5orf66-AS1, AL360182.2 and AL357507.1, were related to poor overall survival. In contrast, CEBPA-DT and AC006033.2 were associated with better survival ***(Figure 3A-G)***.

Co-expression network and enrichment analysis

To explore the mRNAs associated with predict model-related lncRNAs and their potential TF, we integrated the lncRNA and gene data to construct the co-expression network. Firstly, we selected the metastasis-related genes closely associated with seven prognosis-related lncRNAs above reported (R>0.3, p<0.001). As a result, a total of 6 prognosis-related lncRNAs and 24 metastasis-related genes were used to construct the co-expression network ***(Figure 4A)***. The AC006033.2 and AL512422.1 were the most important nodes. To further understand the functions of these genes, we analyzed the interaction between 24 metastasis-related genes and 13 TFs ***(Figure 4B, Table 1)***. Then, the GO analysis was carried out for functional enrichment of the nodes in this co-expression network ***(Figure 4C)***. The results showed several biological processes (BP) and cellular components (CC) pathways markedly enriched. From the BP perspective, the nodes were mainly enriched in “catecholamine metabolic process”, “lymphocyte proliferation”, “mononuclear cell proliferation”, “lymphocyte differentiation” and “leukocyte proliferation”. From the CC perspective, “integral component of synaptic membrane”, “intrinsic component of synaptic membrane” and “glutamatergic synapse” were highlighted.

GSVA Analysis of seven prognosis-related lncRNAs

We performed GSVA to determine the dynamics of biological processes and pathways for Hallmark gene sets based on seven prognosis-related lncRNAs. As Figure 5 showed, “G2M_CHECKPOINT”, “DNA_REPAIR” and “PI3K_AKT_MTOR_SIGNALING” were remarkably activated in the high AL512422.1 group, while the low AL512422.1 group was enriched in “WNT_BETA_CATENIN_SIGNALING” and “KRAS_SIGNALING_DN”. Upregulation of AL008718.3 activated “WNT_BETA_CATENIN_SIGNALING” and “TGF_BETA_SIGNALING”, but downregulation of AL008718.3 led to “HEDGEHOG_SIGNALING” and “PI3K_AKT_MTOR_SIGNALING”. In addition, AC006033.2 high level was significantly enriched for “HYPOXIA”, “APOPTOSIS” and “NOTCH_SIGNALING”, whereas low level triggered “DNA_REPAIR” and “G2M_CHECKPOINT” process. Notably, “GLYCOLYSIS” and “NOTCH_SIGNALING” were all enriched in AL357507.1 and AL360182.2 low groups. For the C5orf66-AS1 low group, “TGF_BETA_SIGNALING”, “HYPOXIA” and “NOTCH_SIGNALING” were enriched. The C5orf66-AS1 high group is related to “WNT_BETA_CATENIN_SIGNALING”. At last, we observed enrichment of “G2M_CHECKPOINT”, “DNA_REPAIR” and “PI3K_AKT_MTOR_SIGNALING” in the CEBPA-DT high group and “WNT_BETA_CATENIN_SIGNALING” in the low group. The top high-frequency enriched pathways were “NOTCH_SIGNALING”, “HYPOXIA”, “WNT_BETA_CATENIN_SIGNALING” and “HEDGEHOG_SIGNALING”.

Correlation of prognosis-related lncRNAs and infiltrating immunocyte fractions

To investigate the diversities between the primary and metastasis OS, 22 infiltrating immunocyte fractions were compared. As Figure 6A showed, the difference between the two groups was insignificant. Next, we analyzed the relationship between seven prognosis-related lncRNAs and 22 infiltrating immune cells ***(Figure 6B)***. The result suggested that AC006033.2 had the strongest relationship with resting dendritic cells, macrophages M0, macrophages M2, activated mast cells, activated neutrophils and memory T cells CD4. AL357507.1 had a close relationship with dendritic cells resting, macrophages M1, neutrophils and plasma cells. CEBPA-DT was associated with monocyte, T cells CD4 naïve, T cells CD8 and T cells regulatory (Tregs). C5orf66-AS1 and AL512422.1 were only related to dendritic cells activated and dendritic cells resting, respectively. On the contrary, for AL360182.2 and AL008718.3, there was no association with immune cells.

The mRNA expression of seven lncRNAs in OS cell lines

We evaluated the mRNA level of seven lncRNAs (AL512422.1, AL008718.3, C5orf66-AS1, AL360182.2, CEBPA-DT, AC006033.2 and AL357507.1) in five OS cell lines. MNNG cell line was a highly OS metastasis cell line, while the other four were weakly OS metastasis cell lines ***(Figure 7)***. The result revealed that AL512422.1 had a higher expression level in U2OS and SJSA-1 cell lines than MNNG ***(Figure 7A)***. A higher mRNA level of AL360182.2 and C5orf66-AS1 is observed in four weakly metastasis cell lines ***(Figure 7E-F)***. Instead, AL008718.3 mRNA level is significantly down-regulated in USO2, SAOS-2, SJSA-1 and HOS cell lines ***(Figure 7B)***. Additionally, the mRNA level of AL357507.1 was only up-regulated in the SAOS-2 cell line ***(Figure 7D)***. Interestingly, even though they were all weak metastasis cell lines, the expression pattern is completely different. AC006033.2 mRNA level is higher in U2OS, SAOS-2 and HOS cell lines, and lower in SJSA-1 cell lines ***(Figure 7C)***. A similar situation occurred with CEBPA-DT, the mRNA level is higher in HOS cell line and lower in SJSA-1 cell line ***(Figure 7G)***.

Discussion

OS is an aggressive malignancy with poor outcomes, especially in patients with metastasis [29]. The overall survival of patients with OS has improved significantly due to the development of advanced treatments. Surgery remains the cornerstone of primary tumor treatment, while adjuvant chemotherapy was the most important determinant of prognosis for patients with metastasis [30,31]. Chemotherapies, such as high-dose methotrexate, doxorubicin, cisplatin and ifosfamide/etoposide, were the most effective agents. However, the rate of metastasis remains high in a significant portion of OS patients [31]. Therefore, to predict or inhibit the metastasis process, it is necessary to identify targets to provide possible diagnosis and therapeutic strategy[32].

Accumulating evidence indicates that lncRNAs are tightly related to tumorigenesis and progression. lncRNAs could play an essential role in various biological processes involved in carcinogenesis, including cell proliferation, cell migration, and tumor metastasis [33–36]. Identifying an effective biomarker lncRNA could be helpful to prevent metastasis. For example, mtlncRNA LIPCAR is a new biomarker for cardiac remodeling that can predict the survival rate of patients with heart failure [37]. Immunoreactive mice showed that targeted therapy of ASncmtRNAs could prevent lung metastasis after melanoma resection [38]. The lentiviral construct targeting ASncmtRNAs could block B16F10 primary tumor proliferation [39]. In vivo studies in isogenic mouse renal cancer models manifested that ASncmtRNAs-targeting ASOs could completely reverse tumor growth [40]. In summary, lncRNA targeting therapy could be a promising therapeutic option for improving the prognosis.

In this study, we identified a new risk-score model using prognosis-related lncRNA, which were generated from a series of bioinformatic analysis, to predict the metastasis of OS patients. All the patients were divided into high and low risk groups based on the median risk score. The patients in the high group have a poor survival rate compared to the low group. This model exhibited a powerful predictive ability through computing the AUC value. The co-expression network showed the association between TF and 24 prognosis-related mRNAs, which had the closest relationship with the seven lncRNAs. Zhong et al. reported that HSF2 was involved in the growth and metastasis of lung cancer [41]. It is worth noting that lungs are the most common site of OS metastasis, and lung metastases are associated with poor prognosis [30]. NRF2 is a transcription factor that modulates the level of reactive oxygen species (ROS), detoxifying agents and antioxidants. The accumulation of NRF2 in the nuclei is closely related to bone metastasis of patients with OS [42]. Besides, Cindy et al. revealed that catecholamines and their receptors could be potential molecular markers for OS progression [43]. In the result of 24 prognosis-related mRNA enrichment, the catecholamine metabolic process and catechol-containing compound metabolic process were mentioned.

We found several overlap pathways among seven lncRNAs enrichment results, which further confirmed the critical biological function of seven lncRNAs. “NOTCH_SIGNALING”, “HYPOXIA”, “WNT_BETA_CATENIN_SIGNALING” and “HEDGEHOG_SIGNALING” were showed with higher frequency. Several researches have proved that the Notch pathway is important in regulating OS metastasis and might be useful for therapeutic targeting in the next few decades[44,45]. Fang et al. reported that the Notch pathway could be pharmacologically inhibited, which was a giant step forward in target therapeutic strategies [46]. CNOT1, cooperating with LMNA, could aggravate OS tumorigenesis through the Hedgehog signaling pathway [47]. In addition, the hypoxia-HIF-1α-CXCR4 pathway plays a crucial role during the migration of human OS cells [48]. Furthermore, NRP2 was also overexpressed in OS cell lines; the depletion of NRP2 through downregulation of the active Wnt-signaling pathway would significantly reduce the tumor burden and metastasis rate in OS cell lines [49]. Additionally, we found three of seven lncRNA were associated with resting dendritic cells. Jones et al. report that IL23 expression and monocyte-derived dendritic cells tend to demonstrate both activating and suppressing effects on cytotoxic T cells, as well as direct impacts on osteoblasts or associated osteoclasts [50]. It is worth noting that dendritic cells would secrete large amounts of osteopontin under hypoxic conditions, which contributes to tumor metastasis [51].

However, there were still some potential limitations in the present study. One limitation is the relatively small sample size, whereas recruitment is still ongoing. Another limitation is further analysis stratified by age to account for metastasis was not performed. In conclusion, we established a new model with high reliability and accuracy to predict the metastasis of OS patients.

Abbreviations

AUC	area under receiver operating characteristic curve
BP	biological processes
CC	cellular components
EMT	epithelial–mesenchymal transition
FDR	false discovery rate
GSEA	Gene set enrichment analysis
GSVA	Gene Set Variation Analysis
KM	Kaplan–Meier
LASSO	least absolute shrinkage and selection operator
lncRNAs	long non-coding RNAs
MsigDB	Molecular Signatures Database
OS	osteosarcoma
ROS	reactive oxygen species
TF	transcription factor
Tregs	T cells regulatory

Declarations

Acknowledgements

Not applicable.

Authors' contributions

Zhang H, Chen GH and Lyu CY designed the study, acquired the data, and wrote the manuscript. Li T and Xu Y reviewed the manuscript. Lyu XJ and Rong C contributed to the Statistical analysis and graphing. Wang YZ and Lyu CY supervised the study. Zhang H and Chen GH contribute equally to this paper.

Funding: This study was supported by National Natural Science Foundation of China (Grant No.81802151), Shandong Provincial Natural Science Foundation of China (Grant No. ZR2016HQ05; ZR2017BH089; ZR2019MH012), General Funding of China Postdoctoral Science Foundation (Grant No.2018M642616) and Qingdao Applied Basic Research Youth Special Project (Grant No.19-6-2- 55-cg).

Availability of data and materials

Publicly available datasets were analyzed in this study. The datasets generated during and/or analyzed during the current study are available from the corresponding author upon reasonable request.

Ethics approval and consent to participate

The study was approved by the Ethical Committee of the Affiliated Hospital of Qingdao University and experiments were performed in accordance with the Ethical Committee's guidelines and regulations.

Consent for publication

All authors have approved the final version of the manuscript and have agreed to submit it to this journal.

Competing interests

The authors declare no conflict of interest with respect to the publication of this article.

References

1. Dorfman HD. Czerniak BJ. Bone cancers. Cancer. 1995;75(S1):203–10.
2. Mirabello L. Troisi RJ, Savage SA. Osteosarcoma incidence and survival rates from 1973 to 2004: data from the Surveillance, Epidemiology, and End Results Program. Cancer. 2009;115(7):1531–43.

3. Unni KK. Inwards CY. Dahlin's bone tumors: general aspects and data on 10,165 cases. *Lippincott Williams & Wilkins*; 2010.
4. Larsson SE. Lorentzon RJ. The incidence of malignant primary bone tumours in relation to age, sex and site: a study of osteogenic sarcoma, chondrosarcoma and Ewing's sarcoma diagnosed in Sweden from 1958 to 1968. J Bone Joint Surg Br. 1974;56(3):534–40.
5. Polednak AP. Primary bone cancer incidence in black and white residents of New York State. Cancer. 1985;55(12):2883–8.
6. Ji J. Hemminki K. Familial risk for histology-specific bone cancers: an updated study in Sweden. Eur J Cancer. 2006 *Sep;*42(14):2343-9.
7. Bacci G. Longhi A, Fagioli F, et al Adjuvant and neoadjuvant chemotherapy for osteosarcoma of the extremities: 27 year experience at Rizzoli Institute, Italy. Cancer. 2005;41(18):2836–45.
8. Link MP. Goorin AM, Miser AW, et al The effect of adjuvant chemotherapy on relapse-free survival in patients with osteosarcoma of the extremity. N Engl J Med. 1986;314(25):1600–6.
9. Rosen G. Caparros B, Huvos AG, et al Preoperative chemotherapy for osteogenic sarcoma: selection of postoperative adjuvant chemotherapy based on the response of the primary tumor to preoperative chemotherapy. Cancer. 1982;49(6):1221–30.
10. Dong J. Liu Y, Liao W. Liu R, *et al.* miRNA-223 is a potential diagnostic and prognostic marker for osteosarcoma. J Bone Oncol. 2016;5(2):74–9.
11. Wang M. Xie R, Si H, et al Integrated bioinformatics analysis of miRNA expression in osteosarcoma. Artif Cells Nanomed Biotechnol. 2017;45(5):936–43.
12. *Di* Fiore R, Drago-Ferrante R. Pentimalli F, *et al.* Let-7d miRNA shows both antioncogenic and oncogenic functions in osteosarcoma-derived 3AB-OS cancer stem cells. J Cell Physiol. 2016;231(8):1832–41.
13. Schwartz CL. Gorlick R, Teot L, et al Multiple drug resistance in osteogenic sarcoma: INT0133 from the Children's Oncology Group. J Clin Oncol. 2007;25(15):2057–62.
14. Gill J. Ahluwalia MK, Geller D, et al New targets and approaches in osteosarcoma. Pharmacol Ther. 2013;137(1):89–99.
15. Shi J. Dong B, Cao J, et al Long non-coding RNA in glioma: signaling pathways. Oncotarget. 2017;8(16):27582.
16. Idogawa M. Ohashi T, Sasaki Y, et al Long non-coding RNA NEAT1 is a transcriptional target of p53 and modulates p53-induced transactivation and tumor-suppressor function. Int J Cancer. 2017;140(12):2785–91.
17. Liang Y. Zhang D, Zheng T, et al lncRNA-SOX2OT promotes hepatocellular carcinoma invasion and metastasis through miR-122-5p-mediated activation of PKM2. Oncogenesis. 2020;9(5):54.
18. Gooding AJ. Zhang B, Jahanbani FK, et al The lncRNA BORG Drives Breast Cancer Metastasis and Disease Recurrence. Sci Rep. 2017;7(1):12698.
19. Wang Z. Yang B, Zhang M, et al *lncRNA Epigenetic Landscape Analysis Identifies EPIC1 as an Oncogenic lncRNA that Interacts with MYC and Promotes Cell-Cycle Progression in Cancer. Cancer Cell.* 2018;*33*(*4*).
20. Kitamura T. Qian BZ, Soong D, et al CCL2-induced chemokine cascade promotes breast cancer metastasis by enhancing retention of metastasis-associated macrophages. J Exp Med. 2015;212(7):1043–59.
21. Li C. Wang S, Xing Z, et al A ROR1-HER3-lncRNA signalling axis modulates the Hippo-YAP pathway to regulate bone metastasis. Nat Cell Biol. 2017;19(2):106–19.
22. Ji P. Diederichs S, Wang W, et al MALAT-1, a novel noncoding RNA, and thymosin β 4 predict metastasis and survival in early-stage non-small cell lung cancer. Oncogene. 2003;22(39):8031–41.
23. Shen L. Chen L, Wang Y, et al Long noncoding RNA MALAT1 promotes brain metastasis by inducing epithelial-mesenchymal transition in lung cancer. J Neurooncol. 2015;121(1):101–8.
24. Ying L. Chen Q, Wang Y, et al Upregulated MALAT-1 contributes to bladder cancer cell migration by inducing epithelial-to-mesenchymal transition. Mol Biosyst. 2012;8(9):2289–94.
25. Fan Y. Shen B, Tan M, et al TGF-β–induced upregulation of malat1 promotes bladder cancer metastasis by associating with suz12. Clin Cancer Res. 2014;20(6):1531–41.
26. Kim K. Jutooru I, Chadalapaka G, et al HOTAIR is a negative prognostic factor and exhibits pro-oncogenic activity in pancreatic cancer. Oncogene. 2013;32(13):1616–25.
27. Zhou Y. Zhang X, Klibanski A. MEG3 noncoding RNA: a tumor suppressor. J Mol Endocrinol. 2012;48(3):R45–53.
28. Peng W. Si S, Zhang Q, et al Long non-coding RNA MEG3 functions as a competing endogenous RNA to regulate gastric cancer progression. J Mol Endocrinol. 2015;34(1):1–10.
29. Hou CH. Lin FL, Hou SM, et al Cyr61 promotes epithelial-mesenchymal transition and tumor metastasis of osteosarcoma by Raf-1/MEK/ERK/Elk-1/TWIST-1 signaling pathway. Mol Cancer. 2014;13(1):1–13.
30. Geller DS. Gorlick R. Osteosarcoma: a review of diagnosis, management, and treatment strategies. Clin Adv Hematol Oncol. 2010;8(10):705–18.
31. Ferguson WS. Goorin AM. Current treatment of osteosarcoma. Cancer Invest. 2001;19(3):292–315.
32. He M. Wang G, Jiang L, et al miR-486 suppresses the development of osteosarcoma by regulating PKC-δ pathway. Int J Oncol. 2017;50(5):1590–600.
33. Li G. Zhang H, Wan X, et al Long noncoding RNA plays a key role in metastasis and prognosis of hepatocellular carcinoma. Biomed Res Int. 2014;2014:780521.
34. Maass PG. Luft FC, Bähring S. Long non-coding RNA in health and disease. J Mol Med (Berl). 2014 *Apr;*92(4):337 – 46.
35. Tripathi V. Shen Z, Chakraborty A, et al Long noncoding RNA MALAT1 controls cell cycle progression by regulating the expression of oncogenic transcription factor B-MYB. PLoS Genet. 2013;9(3):e1003368.
36. Zhang A. Xu M, Mo YY. Role of the lncRNA-p53 regulatory network in cancer. J Mol Cell Biol 2014 *Jun;*6(3):181 – 91.

37. Kumarswamy R. Bauters C, Volkmann I, et al *Circulating long noncoding RNA, LIPCAR, predicts survival in patients with heart failure. Circ Res. 2014 May 9;114(10):1569-75.*
38. Lobos-González L. Silva V, Araya M, et al Targeting antisense mitochondrial ncRNAs inhibits murine melanoma tumor growth and metastasis through reduction in survival and invasion factors. Oncotarget. 2016;7(36):58331.
39. Varas-Godoy M. Lladser A, Farfan N, et al In vivo knockdown of antisense non-coding mitochondrial RNA s by a lentiviral-encoded sh RNA inhibits melanoma tumor growth and lung colonization. Pigment Cell Melanoma Res. 2018;31(1):64–72.
40. Borgna V. Villegas J, Burzio VA, et al Mitochondrial ASncmtRNA-1 and ASncmtRNA-2 as potent targets to inhibit tumor growth and metastasis in the RenCa murine renal adenocarcinoma model. Oncotarget. 2017;8(27):43692.
41. Zhong YH. Cheng HZ, Peng H, et al Heat shock factor 2 is associated with the occurrence of lung cancer by enhancing the expression of heat shock proteins. Oncol Lett. 2016;12(6):5106–12.
42. Zhang J. Wang X, Wu W, et al Expression of the Nrf2 and Keap1 proteins and their clinical significance in osteosarcoma. Biochem Biophys Res Commun. 2016;473(1):42–6.
43. Bandala C. Ávila-Luna A, Gómez-López M, et al Catecholamine levels and gene expression of their receptors in tissues of adults with osteosarcoma. Arch Physiol Biochem. 2019 *Jul* 10:1–7.
44. Tanaka M. Setoguchi T, Hirotsu M, et al Inhibition of Notch pathway prevents osteosarcoma growth by cell cycle regulation. Br J Cancer. 2009;100(12):1957–65.
45. Dai G. Liu G, Zheng D, et al Inhibition of the Notch signaling pathway attenuates progression of cell motility, metastasis, and epithelial-to-mesenchymal transition-like phenomena induced by low concentrations of cisplatin in osteosarcoma. Eur J Pharmacol. 2021 *May* 15;*899*:174058.
46. Fang L. Li B, Yu D, et al Analysis of changes in the expression of Notch1 and HES1 and the prognosis of osteosarcoma patients following surgery. Oncol Lett. 2020;20(4):1–1.
47. Cheng Dd, Li J, Li S, *et al.* CNOT 1 cooperates with LMNA to aggravate osteosarcoma tumorigenesis through the Hedgehog signaling pathway. Mol Oncol. 2017;11(4):388–404.
48. Guo M. Cai C, Zhao G, *et al. Hypoxia promotes migration and induces CXCR4 expression via HIF-1α activation in human osteosarcoma.PLoS One.* 2014 *Mar 11;9(3):e90518.*.
49. Ji T. Guo Y, Kim K, et al Neuropilin-2 expression is inhibited by secreted Wnt antagonists and its down-regulation is associated with reduced tumor growth and metastasis in osteosarcoma. Mol Cancer. 2015;14(1):1–14.
50. Jones KB. Dendritic Cells Drive Osteosarcomagenesis through Newly Identified Oncogene and Tumor Suppressor. Cancer Discov. 2019;9(11):1484–6.
51. Yang M. Ma C, Liu S, et al Hypoxia skews dendritic cells to a T helper type 2-stimulating phenotype and promotes tumour cell migration by dendritic cell-derived osteopontin. Immunology. 2009;128(1 Suppl):e237–49.

Table

Table 1. Transcription factors associated with 24 intersecting mRNAs

Category	Term	Count	%	PValue	Genes	List Total	Pop Hits	Pop Total	Fold Enrichment	Bonferroni	Benjamini	FI
UCSC_TFBS	AHRARNT	17	70.83333	0.006029	GADD45GIP1, CGREF1, MESP1, HMGA1, IKZF1, HOXC13, ITGAL, POU2F2, HOXC12, SORL1, VNN1, HRH2, SFRP5, FAM198B, HRC, NRCAM, SLC27A5	23	9110	20726	1.681583	0.652961	0.601557	0.
UCSC_TFBS	AP4	19	79.16667	0.006875	GADD45GIP1, CGREF1, MESP1, GPR65, IKZF1, HOXC13, ITGAL, POU2F2, HOXC12, SORL1, VNN1, HRH2, MYC, SFRP5, FAM198B, HRC, NRCAM, TLR7, SLC27A5	23	11244	20726	1.522721	0.700987	0.601557	0.
UCSC_TFBS	ARP1	15	62.5	0.018577	GADD45GIP1, CGREF1, MESP1, HMGA1, IKZF1, HOXC13, ITGAL, POU2F2, HOXC12, SORL1, VNN1, HRH2, HRC, TLR7, SLC27A5	23	8167	20726	1.65507	0.96243	0.87694	0.
UCSC_TFBS	NRF2	11	45.83333	0.024629	GADD45GIP1, HRH2, FAM198B, HRC, HMGA1, NRCAM, IKZF1, ITGAL, HOXC12, SORL1, SLC27A5	23	5045	20726	1.964804	0.987273	0.87694	0.
UCSC_TFBS	IK3	14	58.33333	0.025055	GADD45GIP1, MESP1, MMP3, IKZF1, HOXC13, ITGAL, POU2F2, SORL1, MYC, SFRP5,	23	7539	20726	1.673408	0.988211	0.87694	0.

					PDPN, FAM198B, NRCAM, TLR7						
UCSC_TFBS	NF1	12	50	0.043898	GADD45GIP1, CGREF1, HRH2, GPR65, HMGA1, NRCAM, HOXC13, ITGAL, POU2F2, HOXC12, SORL1, SLC27A5	23	6332	20726	1.707765	0.999612	0.935221	0.
UCSC_TFBS	TCF11MAFG	15	62.5	0.047363	CGREF1, MESP1, MMP3, HMGA1, IKZF1, ITGAL, POU2F2, SORL1, VNN1, HRH2, SFRP5, FAM198B, HRC, NRCAM, SLC27A5	23	9047	20726	1.494082	0.999795	0.935221	0.
UCSC_TFBS	HEN1	16	66.66667	0.055655	GADD45GIP1, MESP1, HMGA1, IKZF1, HOXC13, ITGAL, POU2F2, HOXC12, SORL1, VNN1, MYC, SFRP5, HRC, NRCAM, TLR7, SLC27A5	23	10160	20726	1.419103	0.999956	0.935221	0.
UCSC_TFBS	STAT	11	45.83333	0.069174	CGREF1, MYC, SFRP5, PDPN, MMP3, NRCAM, TLR7, IKZF1, ITGAL, HOXC12, SORL1	23	5930	20726	1.671574	0.999996	0.935221	0.
UCSC_TFBS	CEBPB	15	62.5	0.080449	GADD45GIP1, CGREF1, MESP1, IKZF1, HOXC13, ITGAL, POU2F2, HOXC12, SORL1, VNN1, MYC, FAM198B, HRC, NRCAM, TLR7	23	9630	20726	1.40363	1	0.935221	0.
UCSC_TFBS	E47	16	66.66667	0.081955	GADD45GIP1, CGREF1, MESP1,	23	10601	20726	1.360069	1	0.935221	0.

					HMGA1, IKZF1, HOXC13, POU2F2, HOXC12, SORL1, MYC, SFRP5, FAM198B, HRC, NRCAM, TLR7, SLC27A5							
UCSC_TFBS	HSF2	12	50	0.094283	MESP1, CGREF1, VNN1, MYC, PDPN, HRC, NRCAM, IKZF1, ITGAL, HOXC12, SORL1, SLC27A5	23	7109	20726	1.521109	1	0.935221	0.
UCSC_TFBS	RP58	14	58.33333	0.098286	GADD45GIP1, CGREF1, HMGA1, IKZF1, HOXC13, ITGAL, POU2F2, HOXC12, SORL1, PDPN, FAM198B, NRCAM, TLR7, SLC27A5	23	8944	20726	1.410535	1	0.935221	0.

Figures

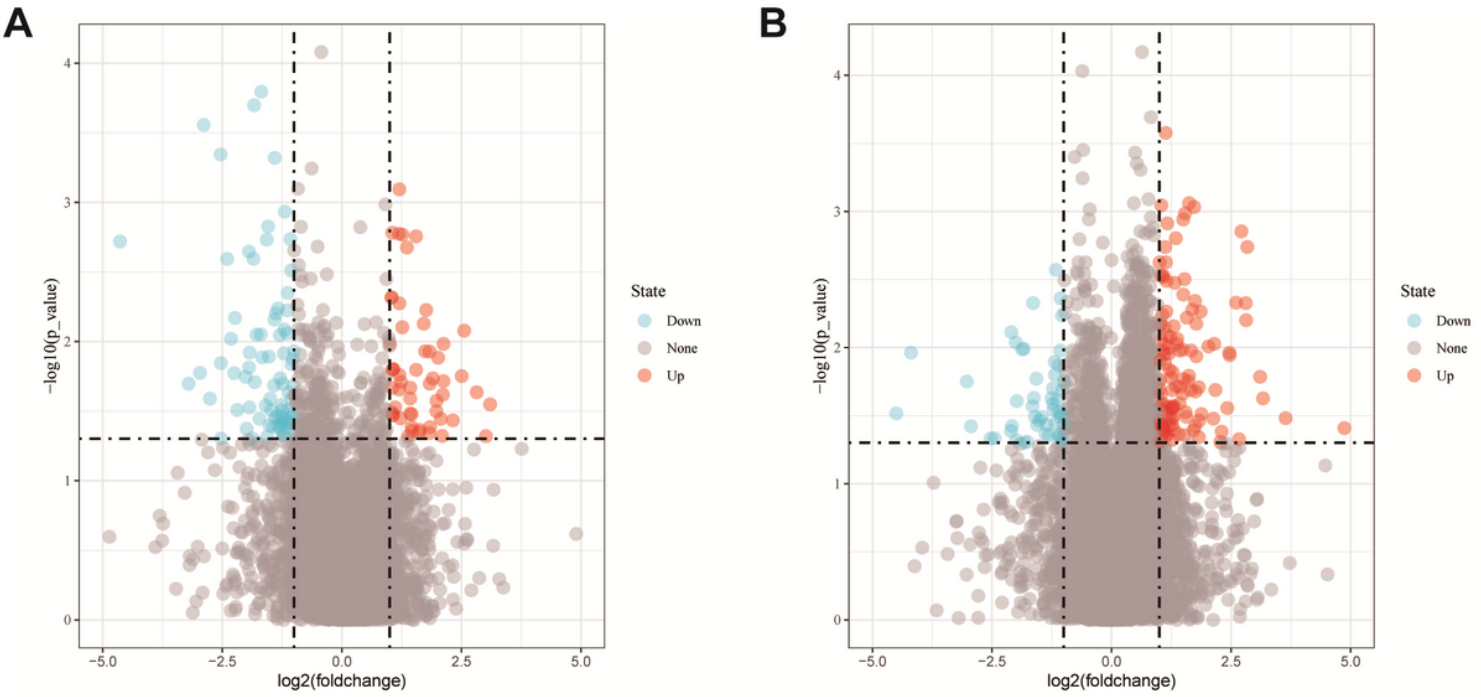

Figure 1

Differential expression profiles. (A) Differential lncRNA between metastatic and non-metastatic OS; (B) Differential mRNA between metastatic and non-metastatic OS.

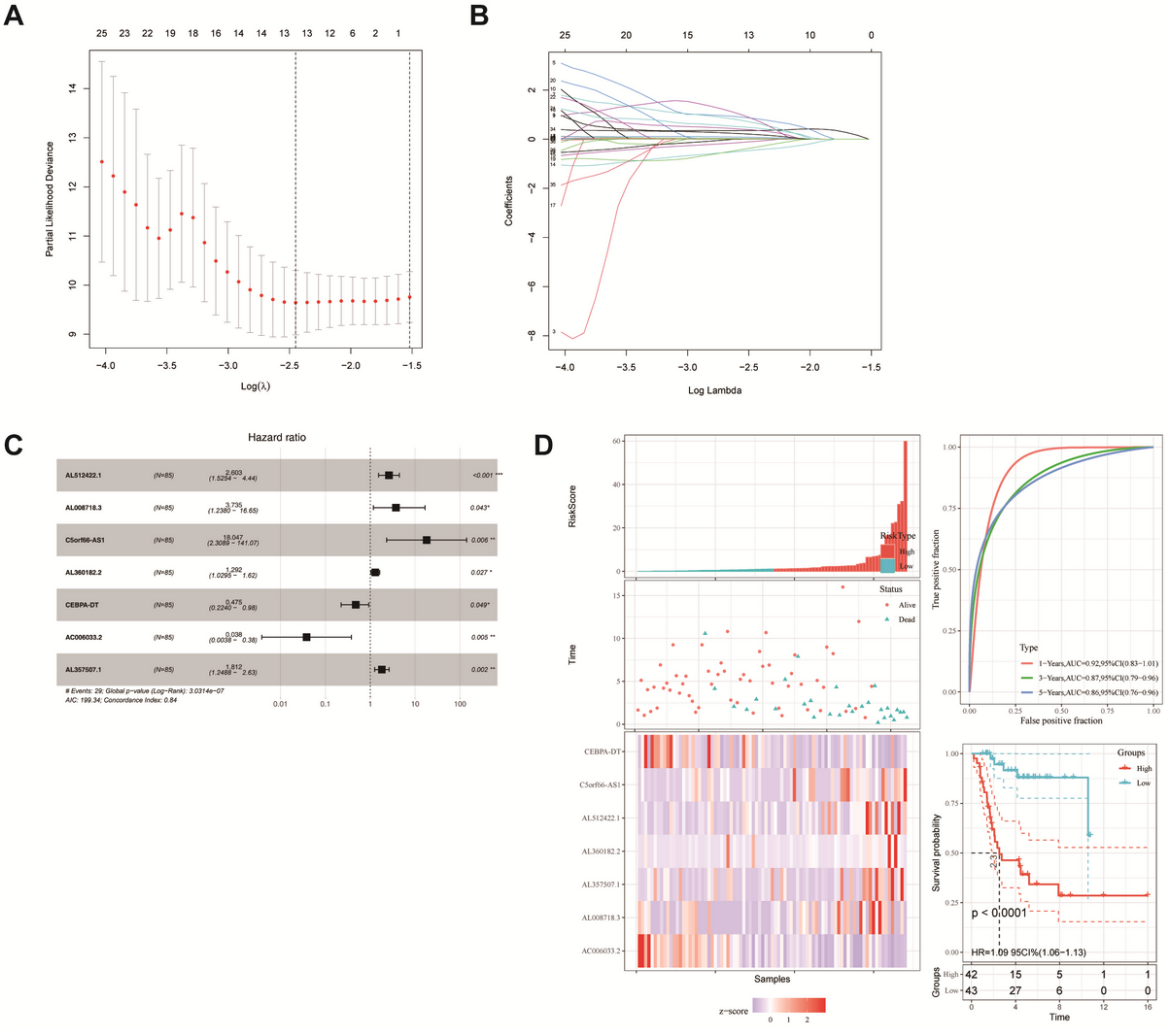

Figure 2

Identification of the prognosis-related lncRNA. (A&B) LASSO coefficient profiles; (C) Multivariate cox analysis of seven model lncRNAs; (D) The risk scores, ROC curve, and Kaplan–Meier curve of patients.

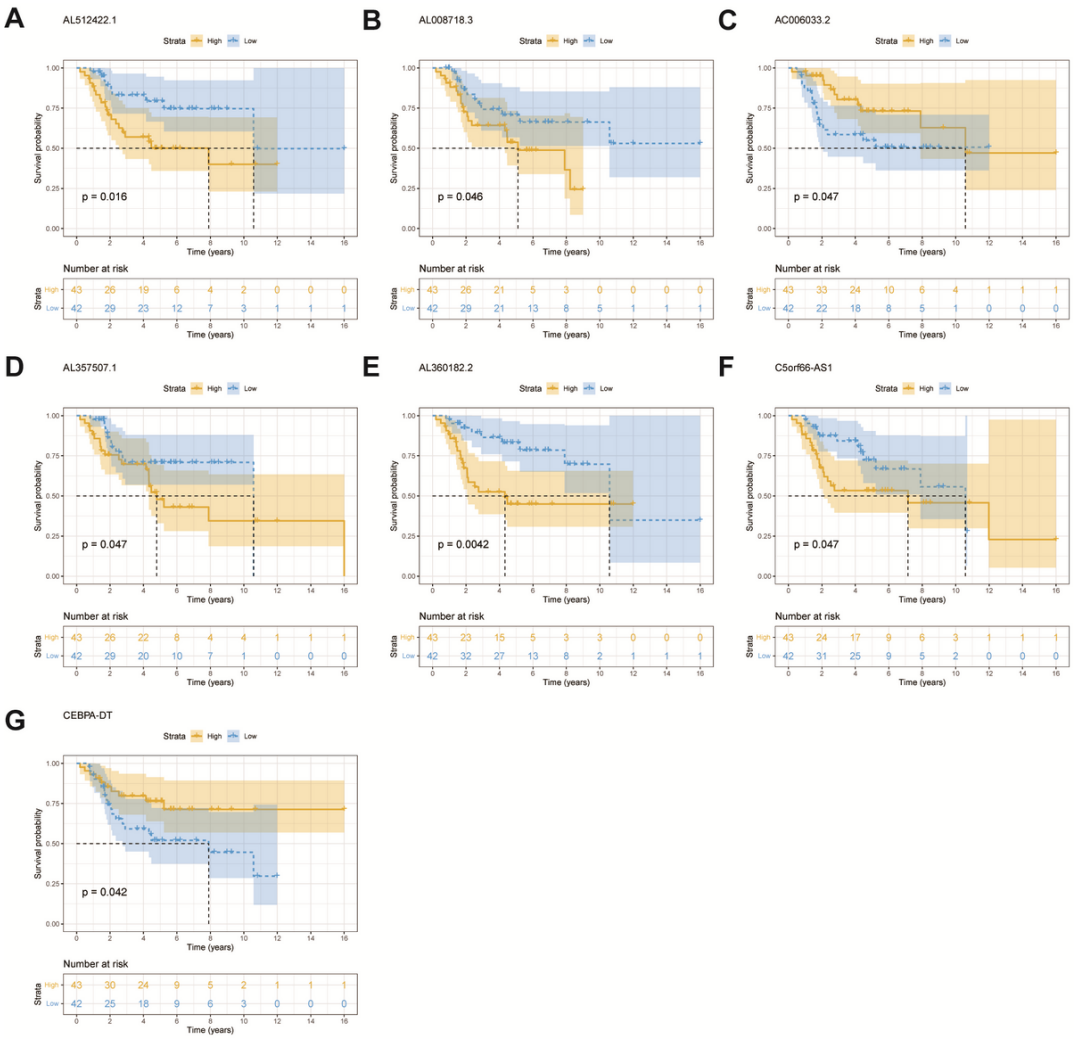

Figure 3

Kaplan–Meier curve of seven prognosis-related lncRNAs.

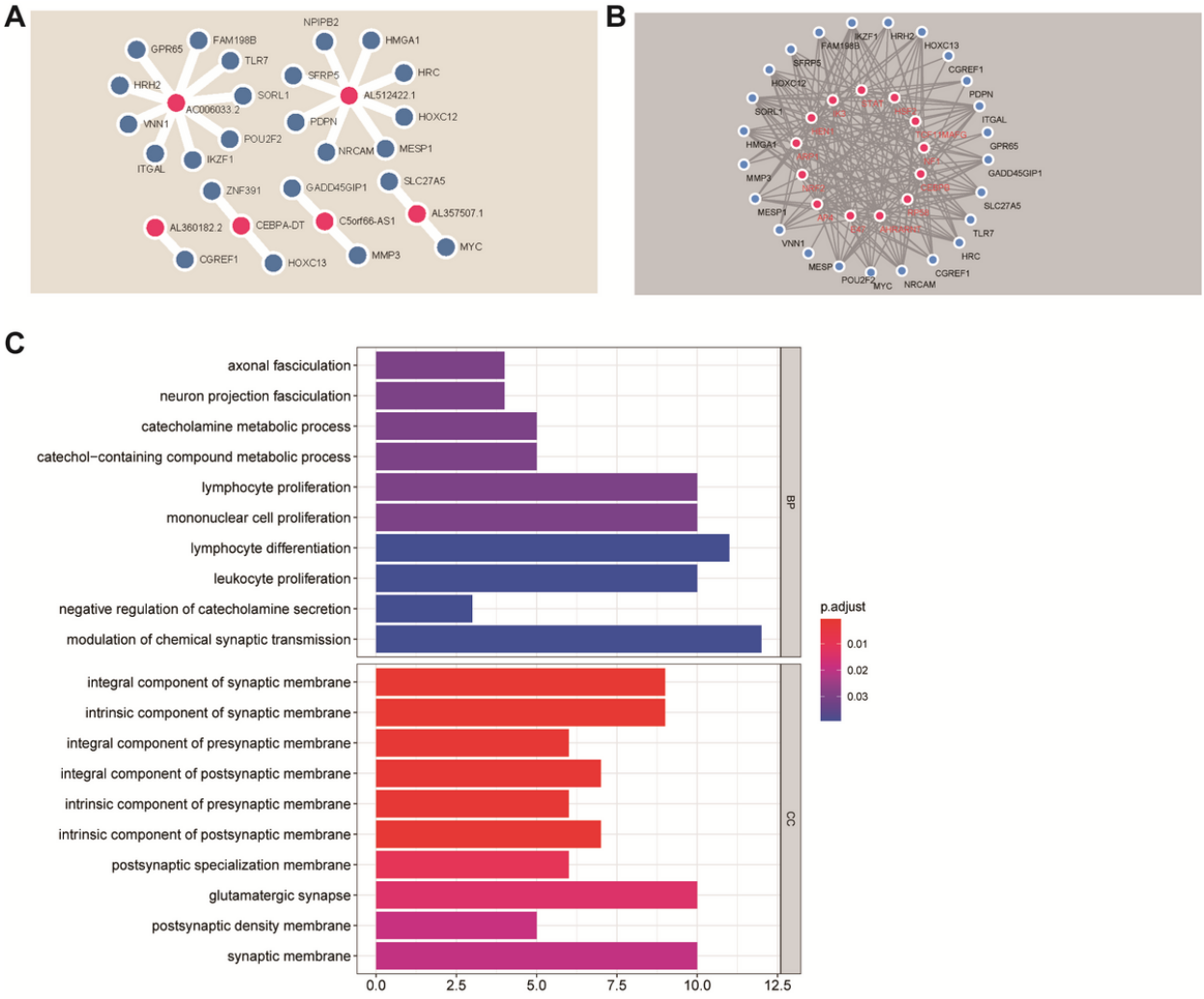

Figure 4

Co-expression network and enrichment analysis. (A) co-expression network of lncRNA and mRNA; (B) co-expression network of mRNA and TF; (C) GO analysis of the genes in co-expression network.

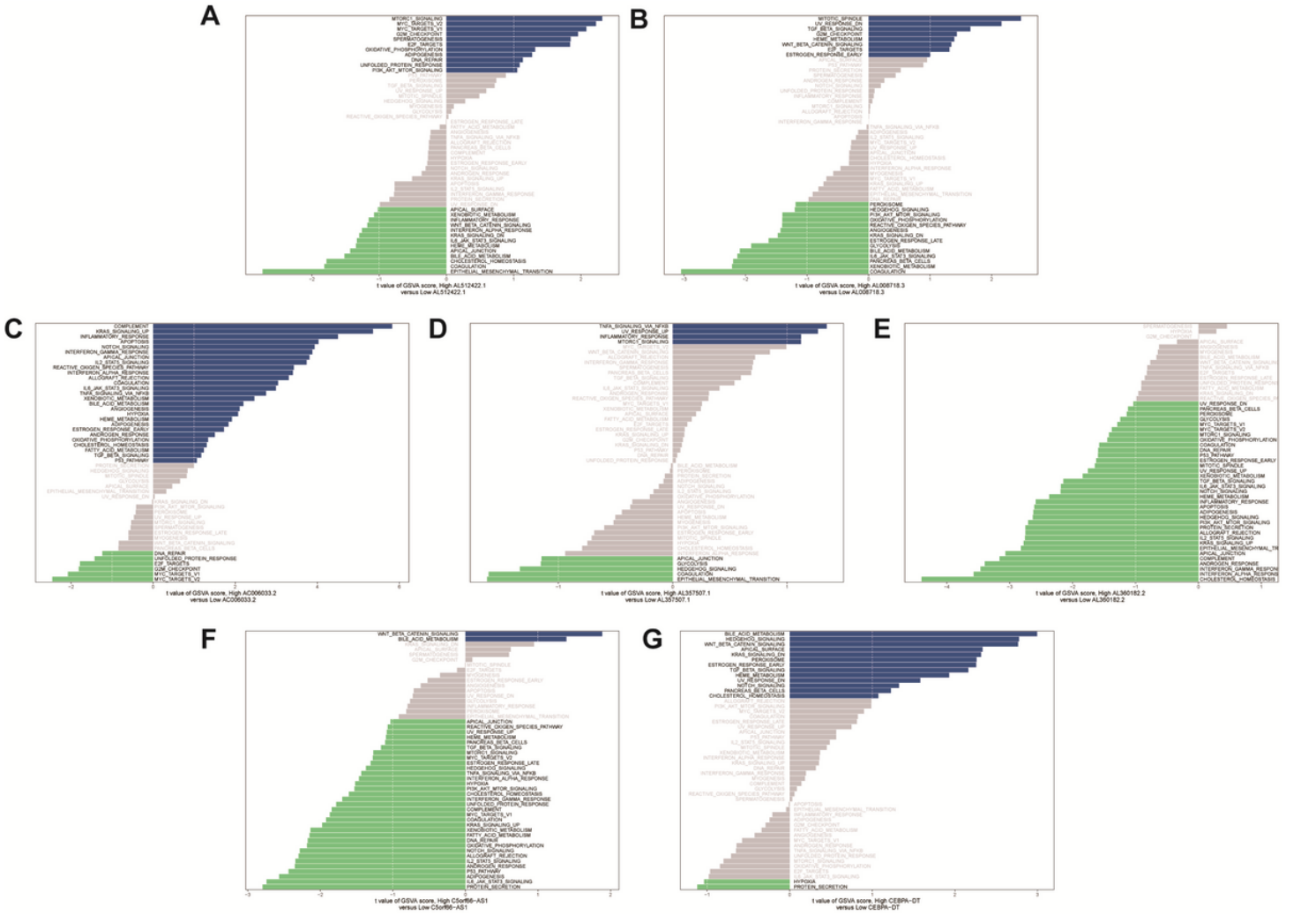

Figure 5

GSVA enrichment analysis of seven prognosis-related lncRNAs.

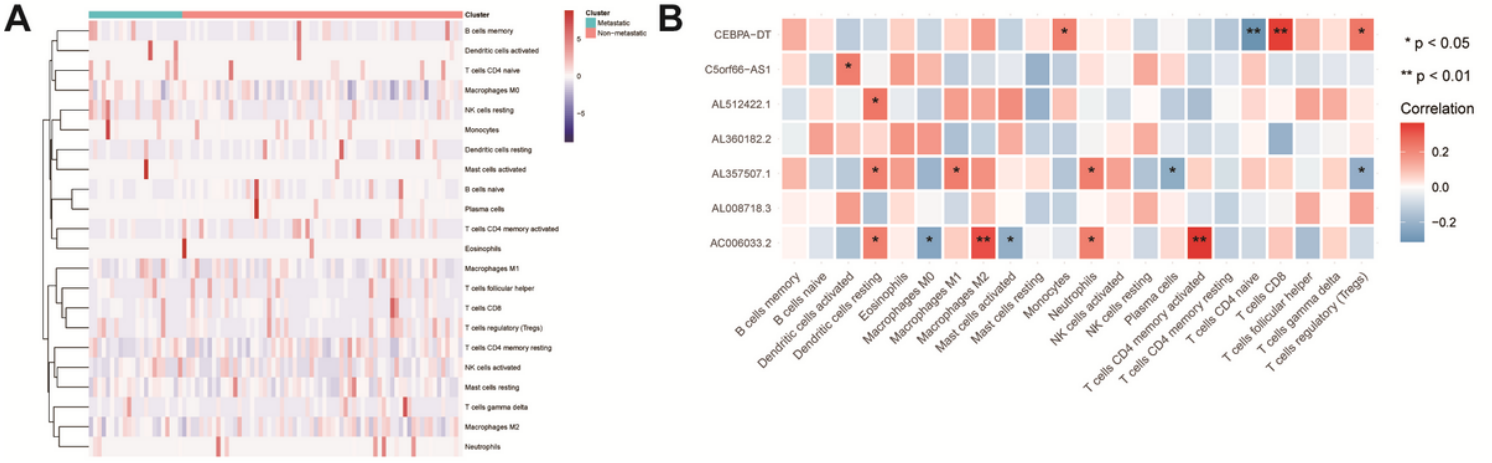

Figure 6

LncRNA and immune analysis. (A) Relationship between high/low group and immune cells; (B) Relationship between seven prognosis-related lncRNAs and immune cells.

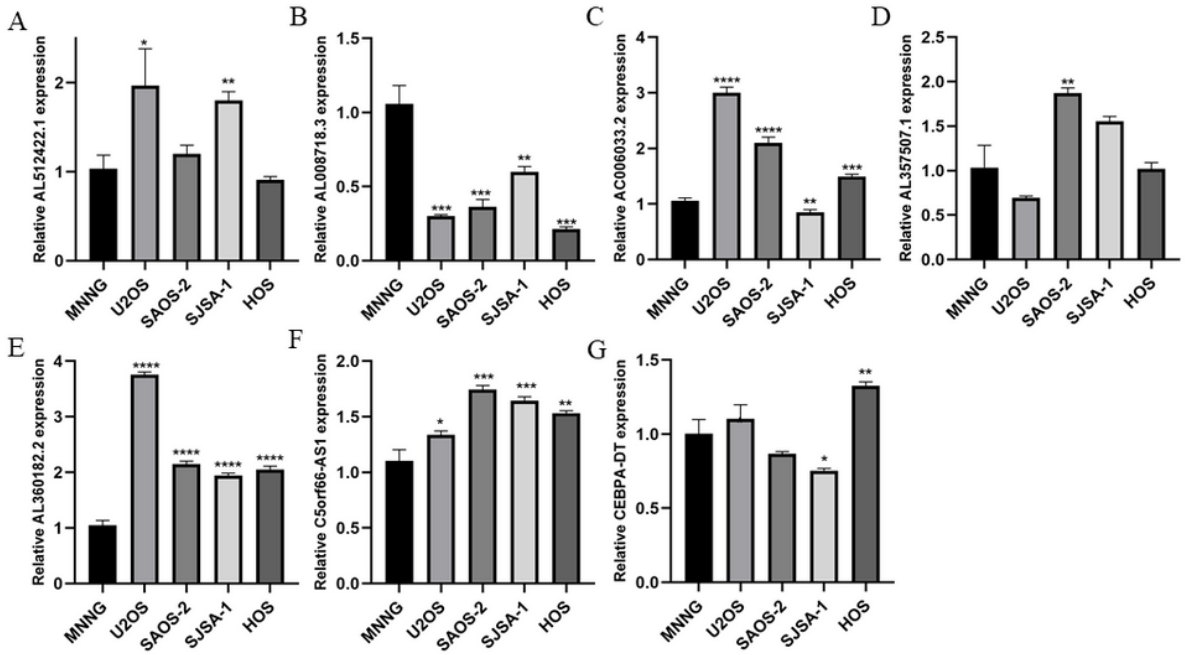

Figure 7

The qPCR result of seven lncRNAs in five OS highly metastasis and weakly metastasis cell lines.

Supplementary Files

This is a list of supplementary files associated with this preprint. Click to download.

- TableS1.docx